J. Fluid Mech. (1975), *vol.* 68, *part* 3, *pp.* 513–535
Printed in Great Britain

Diffraction of oblique waves by an infinite cylinder

By KWANG JUNE BAI
Department of Ocean Engineering, Massachusetts Institute of Technology

(Received 30 August 1973 and in revised form 3 September 1974)

This paper presents a numerical method for solving linearized water-wave problems with oscillatory time dependence. Specifically it considers the diffraction problem for oblique plane waves incident upon an infinitely long fixed cylinder on the free surface. The numerical method is based on a variational principle equivalent to the linearized boundary-value problem. Finite-element techniques are used to represent the velocity potential; and the variational principle is used to determine the unknown coefficients in the solution throughout the fluid domain. To illustrate this method, reflexion and transmission coefficients and the diffraction forces and moment are computed for oblique waves incident upon a vertical flat plate, a horizontal flat plate and rectangular cylinders, where the comparison is made with the existing results by others. Also considered is the associated sinuous forced-motion problem, where comparison is made with the results for a circular cylinder obtained by Bolton & Ursell (1973).

1. Introduction

Small oscillatory motions of an inviscid incompressible fluid with a free surface are described by a boundary-value problem governed by Laplace's equation with a mixed boundary condition on the free surface, a homogeneous Neumann condition on the bottom of the fluid, and appropriate radiation conditions at infinity. Radiation and diffraction problems involving the presence of a floating or submerged body require an additional boundary condition on the body surface as well, generally stating that the normal velocity of the body and fluid are equal. Problems of this type are generally solved by distributing sources and/or dipoles on the body surface and using Green's theorem to obtain an integral equation for the strength of these surface singularities, or alternatively by using sources and higher-order multipole expansions at an interior point of the body, the strengths of these singularities being determined so as to satisfy the body boundary condition. In all cases it is conventional to use the singularities that satisfy the Laplace equation, the free-surface boundary condition, the bottom boundary condition, and the radiation boundary condition. For two- and three-dimensional motions with a fluid of infinite depth, or of finite but constant depth, the required singularities are well known, although of rather complicated analytical form, so that the approach described above corresponds to solving a Fredholm integral equation over the body surface, with a rather complicated kernel function.

In this paper an alternative method is described, based on Bai (1972). A variational principle is used to determine the velocity potential throughout the fluid domain; and the potential is approximated for numerical purposes by a finite-element scheme, using piecewise-continuous two-dimensional polynomials. Thus, in effect, an integral equation over a finite domain with a complicated kernel is replaced by a system of equations over a much larger domain, for the velocity potential throughout the fluid, but with a very much simpler kernel. This approach, described in more detail by Bai (1972) and used therein to solve two-dimensional and axisymmetric three-dimensional problems, will be used here to analyse the diffraction problem for a two-dimensional cylindrical body in the presence of oblique incident waves. The resulting fluid motion is three-dimensional, but sinusoidal in the direction of the body axis, so that the three-dimensional Laplace equation can be reduced to a two-dimensional Helmholtz equation.

Previous studies of oblique wave diffraction by cylindrical obstacles have been made by Lebreton & Margnac (1966), and Black & Mei (1970) for finite depth, and by Garrison (1969), Evans & Morris (1972), and Bolton & Ursell (1973) for infinite depth. Lebreton & Margnac (1966) computed the transmission and reflexion coefficients for a rectangular cylinder on the free surface. Black & Mei (1970) computed the transmission and reflexion coefficients for a rectangular cylinder on the bottom.

Garrison (1969) computed the transmission and reflexion coefficients for a horizontal flat plate of finite beam (i.e. width) on the free surface, whereas Evans & Morris (1972) considered the same problem for a vertical flat plate of finite draft (depth of submergence) piercing the free surface. These two geometries can be regarded as limiting cases of a more general rectangular body geometry of finite beam and draft; we shall consider this more general case, and compute the reflexion and transmission coefficients and the diffraction forces and moment for various angles of the obliquely incident waves, comparing with the two limiting cases of vertical and horizontal flat plates. Another special case is the diffraction problem of a wave normally incident on an infinite rectangular cylinder (i.e. the beam-waves case, which is strictly two-dimensional), which has been treated for finite depth by Lebreton & Margnac (1966) and Mei & Black (1969). As a method of solution, Black & Mei (1970) also used a variational technique based on Schwinger's variational principle, which gives only the far-field solution, whereas the variational scheme to be used in this paper gives the potential throughout the domain. We shall also consider the above-mentioned more general case in water of finite depth. Bolton & Ursell (1973) considered a closely related problem, of the waves generated by a circular cylinder oscillating with a vertical heave amplitude that is sinuous, or sinusoidal along the body axis. This problem is related by the Haskind relations to the determination of the diffraction force, for oblique incident waves; and we shall compare the results of Bolton & Ursell (1973) with corresponding calculations based on the present numerical scheme.

2. Formulation of the problem

The co-ordinate system is right-handed and rectangular. The y axis is directed oppositely to the force of gravity; and the x, z plane coincides with the free surface when the fluid is at rest. We assume that the fluid is inviscid, incompressible, and its motion irrotational; hence there exists a velocity potential. Furthermore, surface tension is neglected, and we assume that the motion is sinusoidal in time as well as along the cylinder (z axis).

A simple harmonic plane wave of small amplitude is obliquely incident upon an infinitely long fixed cylinder, the direction of the wave propagation making an angle α with the x axis. We assume that the linearized velocity potential

$$\Phi(x, y, z, t)$$

has a form
$$\Phi(x, y, z, t) = \mathrm{Re}\,[\phi(x, y) \exp(iK_z z - i\sigma t)], \tag{2.1}$$

where K_z is the wavenumber component in the z direction, and σ is the frequency. Then $\Phi(x, y, z, t)$ satisfies

$$\left(\frac{\partial^2}{\partial x^2} + \frac{\partial^2}{\partial y^2} + \frac{\partial^2}{\partial z^2}\right) \Phi(x, y, z, t) = 0 \tag{2.2}$$

in the fluid,
$$\left(\frac{\partial}{\partial y} - K_0\right) \Phi = 0 \tag{2.3}$$

on the free surface,
$$\frac{\partial}{\partial n} \Phi = 0 \tag{2.4}$$

on the body,
$$\frac{\partial}{\partial n} \Phi = 0, \quad y = -H \quad \text{or} \quad y = -\infty \tag{2.5}$$

on the bottom. $K_0 = \sigma^2/g$; and H is the depth of water. Finally, we have to impose a radiation condition at $|x| = \infty$, to make the solution unique.

To solve the above problem, it is convenient to assume that

$$\Phi(x, y, z, t) = \Phi_I + \Phi_D. \tag{2.6}$$

Φ_I and Φ_D are, respectively, the potentials for the incident and the diffracted waves. The incident-wave potential Φ_I of unit wave amplitude is

$$\Phi_I = \mathrm{Re}\left\{\frac{g}{\sigma} \frac{\cosh[K(y+H)]}{\cosh(KH)} \exp(iK_x x + iK_z z - i\sigma t)\right\}, \tag{2.7}$$

where
$$K_0 = K \tanh(KH), \quad K_z = K \sin\alpha, \quad K_x = K \cos\alpha.$$

Then the boundary condition on the body (2.4) becomes

$$\frac{\partial}{\partial n} \Phi_D = -\frac{\partial \Phi_I}{\partial n}. \tag{2.8}$$

As a radiation condition, we require that the diffracted-wave potential $\Phi_D(x, y, z, t)$ has an asymptotic behaviour, as $x \to \mp\infty$,

$$\Phi_D \sim \mathrm{Re}\left[\frac{g}{\sigma} \frac{\cosh[K(y+H)]}{\cosh(KH)} \begin{Bmatrix} R \\ T \end{Bmatrix} \exp(\pm iK_x x + iK_z z - i\sigma t)\right]. \tag{2.9}$$

R and T are respectively the reflexion and transmission coefficients. When we precipitate the t- and z-dependence of the diffracted-wave potential $\Phi_D(x, y, z, t)$ in the above formulation, by using the relations (2.1) and (2.6), (2.2) and (2.5) are reduced to

$$\left(\frac{\partial^2}{\partial x^2}+\frac{\partial^2}{\partial y^2}-K_z^2\right)\phi_D(x,y)=0 \tag{2.10}$$

in the fluid,

$$\left(\frac{\partial}{\partial y}-K_0\right)\phi_D=0 \tag{2.11}$$

on $y=0$,

$$\frac{\partial}{\partial n}\phi_D=-\frac{\partial}{\partial n}\phi_I \tag{2.12}$$

on the body,

$$\frac{\partial}{\partial n}\phi_D=0, \quad y=-H \quad \text{or} \quad y=-\infty, \tag{2.13}$$

where

$$\Phi_I=\mathrm{Re}\{\phi_I(x,y)\exp(iK_z z-i\sigma t)\},$$
$$\Phi_D=\mathrm{Re}\{\phi_0(x,y)\exp(iK_z z-i\sigma t)\}.$$

Finally we have, as a radiation condition at infinity, from (2.9),

$$(\partial/\partial x \mp iK_x)\phi_D \to 0 \quad \text{as} \quad x \to \pm\infty. \tag{2.14}$$

It should be noted that (2.14) reduces to a rigid-vertical-wall condition

$$\partial\phi_D/\partial x=0$$

when the angle of incidence α becomes $\frac{1}{2}\pi$.

When we are interested in the forces exerted on the fixed body in an incident wave, we can also compute the forces by solving a forced-motion problem and using the Haskind relation, instead of solving the diffraction problem formulated above. We shall consider here a forced-motion problem, which is very closely related to the diffraction problem formulated above. Let the forced motion on an infinitely long cylinder be expressed as

$$\frac{\partial}{\partial n}\Phi=\mathrm{Re}\{V_n(x,y)\exp(iK_z z-i\sigma t)\}. \tag{2.15}$$

This expresses, in general, a combination of motions of the three degrees of freedom (heave, sway, roll) in the x, y plane which is sinusoidal along the z axis, as well as in time t. Then we obtain, from (2.1) and (2.15),

$$\phi_n(x,y)=V_n(x,y). \tag{2.16}$$

Once we assume that the local disturbance of the body decays sufficiently at a finite distance X_R, from the moving body, we can apply the radiation condition (2.14) on $x=\pm X_R$, for an approximate scheme. Now we have a well-posed boundary-value problem defined in a finite domain after truncating the infinite boundary, as shown in figure 1, where C_B, C_F, C_R, C_D are, respectively, the body boundary, the free surface, radiation boundary and the bottom boundary. An analysis of the behaviour of the local disturbance to find an optimum distance X_R, on which the radiation condition is to be imposed, is given in appendix A.

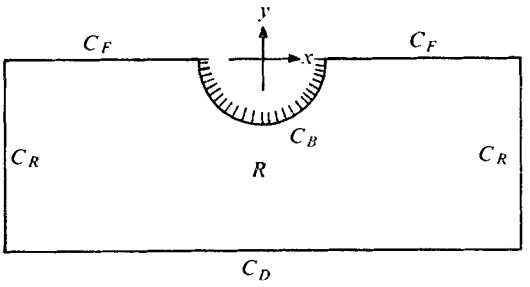

FIGURE 1. The finite domain after truncating the infinite boundaries.

When we write down the final formulation again for the numerical scheme to be discussed in §3, by dropping the subscript D from ϕ_D, we have, for a diffraction or forced-motion problem,

$$\left(\frac{\partial^2}{\partial x^2}+\frac{\partial^2}{\partial y^2}-K_z^2\right)\phi(x,y)=0 \quad \text{in} \quad R, \tag{2.17}$$

$$\frac{\partial}{\partial n}\phi-K_0\phi=0 \quad \text{on} \quad C_F, \tag{2.18}$$

$$\frac{\partial}{\partial n}\phi=V_n(x,y) \quad \text{on} \quad C_B \tag{2.19}$$

($V_n=-\partial\phi_I/\partial n$, for a diffraction problem),

$$\frac{\partial\phi}{\partial n}=0 \quad \text{on} \quad C_D, \tag{2.20}$$

$$\partial\phi/\partial n-iK_x\phi=0 \quad \text{on} \quad C_R(x=\pm X_R). \tag{2.21}$$

3. Variational method

Let us consider a boundary-value problem described for a real function $\phi(x,y)$ as

$$(\nabla^2-K_z^2)\,\phi(x,y)=0 \quad \text{in} \quad R, \tag{3.1}$$

with the mixed-type boundary condition

$$\phi_n+p(x,y)\,\phi-q(x,y)=0 \quad \text{on} \quad C. \tag{3.2}$$

$p(x,y)$ and $q(x,y)$ are known real functions. Instead of solving directly the boundary-value problem (3.1) and (3.2), we can avail ourselves of the theory of the calculus of variations to find the function ϕ, which minimizes the associated functional.To construct the functional for the problem, we introduce a variation $\delta\phi$, and integrate (3.1) in R and (3.2) on C, after multiplying by $\delta\phi$. Then we obtain

$$\iint_R -(\nabla^2-K_z^2)\,\phi\,\delta\phi\,dx\,dy+\int_C(\phi_n+p\phi-q)\,\delta\phi\,ds=0. \tag{3.3}$$

If we make use of the Green's theorem in the first integral in (3.3) and of the relation $\nabla\delta\phi = \delta\nabla\phi$, the left-hand side of (3.3) becomes

$$\iint_R (\nabla\phi\nabla\delta\phi + K_z^2\phi\delta\phi)\,dx\,dy + \int_C (p\phi - q)\,\delta\phi\,ds$$
$$= \delta\left\{\iint_R \tfrac{1}{2}(|\nabla\phi|^2 + K_z^2\phi^2)\,dx\,dy + \int_C (\tfrac{1}{2}p\phi^2 - q\phi)\,ds\right\}. \quad (3.4)$$

We define the functional $F\{\phi\}$ as

$$F\{\phi\} = \iint_R \tfrac{1}{2}\{|\nabla\phi|^2 + K_z^2\phi^2\}\,dx\,dy + \int_C \tfrac{1}{2}p\phi^2 - q\phi)\,ds. \quad (3.5)$$

Then we have
$$\delta F\{\phi\} = 0. \quad (3.6)$$

Since (3.6) is equivalent to (3.1) and (3.2), we shall use (3.6).

The classical variational principle discussed above cannot readily be applied to the problem described in § 2, since $\phi(x, y)$, $p(x, y)$ and $q(x, y)$ in (3.1) and (3.2) are complex functions in the formulation given in (2.17)–(2.21). We shall discuss two different formal approaches, to use the variational principle for our problem. As a first approach, we can separate the real and imaginary parts in the formulation of (2.17)–(2.21), and obtain two sets of equations coupled by the radiation condition at the radiation boundary $x = \pm X_R$:

$$\left(\frac{\partial}{\partial x^2} + \frac{\partial^2}{\partial y^2} - K_z^2\right)\phi_i = 0 \quad (i = 1, 2) \quad \text{in} \quad R, \quad (3.7a, b)$$

$$\frac{\partial}{\partial n}\phi_i - K_0\phi_i = 0 \quad (i = 1, 2) \quad \text{on} \quad C_F, \quad (3.8a, b)$$

$$\left.\begin{aligned} \frac{\partial}{\partial n}\phi_i &= V_n^i \\ \frac{\partial}{\partial n}\phi_i &= -\frac{\partial}{\partial n}\phi_I^i \end{aligned}\right\} \quad (i = 1, 2) \quad \text{on} \quad C_B \quad (3.9a, b)$$

(the lower equation is for the diffraction problem),

$$\frac{\partial\phi_i}{\partial n} = 0 \quad (i = 1, 2) \quad \text{on} \quad C_D, \quad (3.10a, b)$$

$$\frac{\partial\phi_1}{\partial n} = -K_x\phi_2, \quad \frac{\partial\phi_2}{\partial n} = K_x\phi_1 \quad \text{on} \quad C_R(x = \pm X_R), \quad (3.11a, b)$$

where
$$\phi(x, y) = \phi_1(x, y) + i\phi_2(x, y),$$
$$V_n(x, y) = V_n^1(x, y) + iV_n^2(x, y),$$
$$\phi_I(x, y) = \phi_I^1 + i\phi_I^2.$$

If we treat the radiation condition (3.11) as if the normal velocity were given, as in (3.9), and use (3.1), (3.2) and (3.5), we obtain the coupled functionals

$$F_1\{\phi_1\} = \iint_R (\tfrac{1}{2}|\nabla\phi_1|^2 + \tfrac{1}{2}K_z^2\phi_1^2)\,dx\,dy + \oint_C (\tfrac{1}{2}p\phi_1^2 - q\phi_1)\,ds$$
$$= \iint_R (\tfrac{1}{2}|\nabla\phi_1|^2 + \tfrac{1}{2}K_z^2\phi_1^2)\,dx\,dx - \int_{C_F} \tfrac{1}{2}K_0\phi_1^2 ds - \int_{C_B} V_n^1\phi_1 ds$$
$$+ \int_{C_R} K_x\phi_2\phi_1 ds, \quad (3.12a)$$

$$F_2\{\phi_2\} = \iint_R (\tfrac{1}{2}|\nabla\phi_2|^2 + \tfrac{1}{2}K_z^2\phi_2^2)\,dx\,dy + \oint (\tfrac{1}{2}p\phi_2^2 - q\phi_2)\,ds$$

$$= \iint_R (\tfrac{1}{2}|\nabla\phi_2|^2 + \tfrac{1}{2}K_z^2\phi_2^2)\,dx\,dy - \int_{C_F} \tfrac{1}{2}K_0\phi_2^2 ds - \int_{C_B} V_n^2\phi_2 ds$$

$$- \int_{C_R} K_x\phi_1\phi_2 ds. \quad (3.12b)$$

These are positive definite for each function ϕ_1 and ϕ_2, respectively. It is easy to show that the solutions ϕ_1 and ϕ_2 of the coupled problems

$$\delta F_i\{\phi_i\} = 0 \quad (i = 1, 2) \qquad (3.13a, b)$$

are the real and imaginary parts of the solution of the problem described in (2.17)–(2.21).

The second approach, which is neater formally than the first, is to extend all the procedures from (3.1)–(3.6) to the complex functions $\phi(x, y)$, $p(x, y)$, $q(x, y)$ and the complex functional $F\{\phi\}$. Since Green's theorem remains the same when we extend it to the complex functions, we can simply define the associated complex functional $F\{\phi\}$ in (3.14) from (3.5):

$$F\{\phi\} = \iint_R (\tfrac{1}{2}\nabla\phi\nabla\phi + \tfrac{1}{2}K_z^2\phi^2)\,dx\,dy + \oint_C (\tfrac{1}{2}p\phi^2 - q\phi)\,ds. \qquad (3.14)$$

When we use this complex functional $F\{\phi\}$ in (3.14), we have to change the statement 'to find the minimum of the functional', mentioned earlier 'to find a stationary point rather than a minimum'. The complex function ϕ in

$$\delta F\{\phi\} = 0, \qquad (3.15)$$

which causes the first variation of F to be zero, is the solution to (3.1) and (3.2), where $\phi(x, y)$, $p(x, y)$ and $q(x, y)$ are complex. With appropriate choices of $p(x, y)$ and $q(x, y)$, the associated complex functional $F\{\phi\}$ for our problem simply becomes

$$F\{\phi\} = \iint_R [\tfrac{1}{2}(\nabla\phi)^2 + \tfrac{1}{2}K_z^2\phi^2]\,dx\,dy - \int_{C_F} \tfrac{1}{2}K_0\phi^2 ds - \int_{C_B} V_n\phi ds - i\int_{C_R} \tfrac{1}{2}K_x\phi^2 ds. \qquad (3.16)$$

One can also obtain two real functionals, the real and imaginary parts of the complex functional, defined in (3.14):

$$F_3\{\phi_1, \phi_2\} = \iint_R \tfrac{1}{2}\{(\nabla\phi_1)^2 + K_z^2\phi_1^2 - (\nabla\phi_2)^2 - K_z^2\phi_z^2\}\,dx\,dy$$

$$+ \oint_C \{\tfrac{1}{2}p_1(\phi_1^2 - \phi_2^2) - p_2\phi_1\phi_2 - q_1\phi_1 + q_2\phi_2\}\,ds, \quad (3.17a)$$

$$F_4\{\phi_1, \phi_2\} = \iint_R (\nabla\phi_1\nabla\phi_2 + K_z^2\phi_1\phi_2)\,dx\,dy$$

$$+ \oint_C \{\tfrac{1}{2}p_2(\phi_1^2 - \phi_2^2) + p_1\phi_1\phi_2 - q_2\phi_1 - q_1\phi_2\}\,ds. \quad (3.17b)$$

Here $\phi = \phi_1 + i\phi_2$, $p = p_1 + ip_2$, $q = q_1 + iq_2$ and $F\{\phi\} = F_3\{\phi_1, \phi_2\} + iF_4\{\phi_1, \phi_2\}$. When we set the first variation of (3.17a, b) to zero, we obtain

$$\delta F_3\{\phi_1, \phi_2\} = 0, \quad \delta F_4\{\phi_1, \phi_2\} = 0. \tag{3.18a, b}$$

It is easy to show that the solutions of either (3.18a, b) are the real and imaginary parts of the solution of the differential equations in (3.1) and (3.2), with $\phi(x, y)$, $p(x, y)$ and $q(x, y)$ complex functions.

Also, one can use any one of the four sets of functionals constructed so far (i.e. the two real coupled functionals defined in (3.12a, b), a single complex functional $F\{\phi\}$ defined in (3.14), a single real functional $F_3\{\phi_1, \phi_2\}$ and a single real functional $F_4\{\phi_1, \phi_2\}$ defined, respectively, in (3.17a, b)). It is not surprising to have four choices for the associated functionals of the original problem, if one remembers that the associated functional for a given differential equation is not unique. The functionals $F_1\{\phi_1\}$ and $F_2\{\phi_2\}$ in (3.12a, b) are positive definite, as mentioned before, whereas the functionals $F_3\{\phi_1, \phi_2\}$ in (3.17a) and $F_4\{\phi_1, \phi_2\}$ in (3.17b) are indefinite.

As mentioned in §1, the equivalence of differential equations to variational problems is basic to the choice of the computational scheme. One significant difference between the functional method and the differential equation is the fact that the expressions for the associated functionals in (3.12a, b), (3.14), (3.17a, b) involve no second derivatives, owing to the integrations by parts used to construct these functionals. (More specifically, Green's theorem is used here.) It follows that the functionals will be well defined if only the first derivative of the function, rather than the second, is required to be bounded. Therefore the class of admissible functions, in the problem to find the stationary point, is enlarged to a space bigger than that for the original differential equations. We now have the advantage, while searching for the stationary point of the functional, of being permitted to try functions outside the class of those originally admissible. In practice, this means that we can now try continuous functions whose first derivatives are only piecewise continuous. In other words, the first derivative can have finite discontinuities at the juncture points between adjacent elements. It is very easy to construct functions that satisfy the above requirements; we shall discuss this point in §4.

There exist rigorous mathematical treatments of the convergence, and error, of a positive-definite convex functional; the convergence proof for the complex functional $F\{\phi\}$ in (3.14) is more difficult. It is beyond the scope of this paper to give a rigorous proof of convergence for the complex functional: one can find a proof, along with an estimate of the error involved, in Strang & Fix (1973). A rigorous treatment of the convergence of the indefinite functional (3.17) is not at present available (Strang 1974, private communication).

4. Finite-element discretization

In §4 a brief description is given of the finite-element discretization, by which the variational form constructed in §3 can be reduced into an operational form. The complex functional $F\{\phi\}$ of a single complex function ϕ defined in (3.14)

is treated, with the goal of developing a numerical procedure for finding the function $\phi(x, y)$ that makes the functional stationary. The other functionals, single or coupled, can be treated by the same procedure; they result in identical matrix equations. The corresponding treatment of the coupled functionals similar to (3.12) is in Bai (1972).

Let the region occupied by fluid, up to the place at which the radiation condition is to be imposed, be subdivided by lines into a (not necessarily rectangular) grid. Each connected piece within the subdivision will be called an 'element'. We suppose $\phi(x, y)$ to be a function that is continuous and bounded† (but see the discussion in § 5) in the subdivided region. One of the important steps in the procedure is the introduction of a set of interpolation functions $N_i(x, y)$, $i = 1, \ldots, \eta$, associated with *each* element, of such a character that ϕ can be approximated as a sum of them, each multiplied by the value of ϕ at, say, a node of the grid associated with the element (ϕ_i at the ith node). However, these values of ϕ_i need not be nodal values of ϕ, but may be other values (parameters) characterizing ϕ in the element; for our numerical scheme requires finding the stationary point of a functional represented in integral form. We write the set of interpolation functions as a row vector

$$[N] = [N_1, N_2, \ldots, N_n], \tag{4.1}$$

and the set of nodal values as a column vector

$$\{\phi\}^e = [\phi_1^e, \phi_2^e, \ldots, \phi_n^e]^T \tag{4.2}$$

in an n-node element. The superscript e on $\{\phi\}$, or on $\phi_1, \phi_2, \ldots, \phi_n$, means that these values are considered in an individual element. We may then approximate ϕ in each element by the sum

$$\phi = [N]\{\phi\}^e. \tag{4.3}$$

Although in our actual computations an eight-node quadrilateral element was used, we shall give for illustration the example of an eight-node square element. We consider a square element with one node at each vertex, and one at the mid-point of each side, as shown in figure 2. The co-ordinates of each node and nodal numbers are shown also in figure 2. If we want to interpolate a function $\phi(x, y)$ in this element, and if it is known at the eight nodes, we can assume it can be expressed as

$$\phi(x, y) = C_1 + C_2 x + C_3 y + C_4 x^2 + C_5 y^2 + C_6 xy + C_7 x^2 y + C_8 xy^2. \tag{4.4}$$

C_i ($i = 1, \ldots, 8$) are the coefficients to be determined. These can be determined if we use the eight conditions

$$\phi(x, y)|_{\substack{x=x_i \\ y=y_i}} = \phi_i \quad (i = 1, 8). \tag{4.5}$$

(x_i, y_i) are the co-ordinates of the ith node. From (4.4) and (4.5) we obtain

$$\phi(x, y) = \sum_{i=1}^{8} \phi_i N_i(x, y), \tag{4.6}$$

† When the gradient of the function becomes unbounded at a point on the boundary, we can introduce a more sophisticated interpolation function in the near field of the singularity. The problem of a square-root singularity has been treated by Tong & Pian (1973) in an elastic crack analysis.

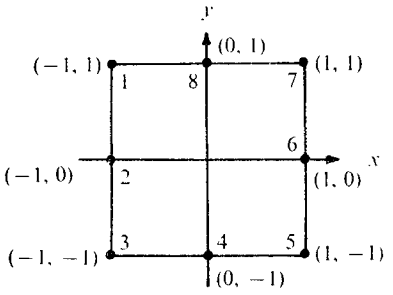

FIGURE 2. An eight-node square element.

where
$$\left.\begin{aligned}
N_1(x,y) &= \tfrac{1}{4}\{(1-x)(1+y)-(1-x^2)(1+y)-(1-x)(1-y^2)\},\\
N_2(x,y) &= \tfrac{1}{2}(1-x)(1-y^2),\\
N_3(x,y) &= \tfrac{1}{4}\{(1-x)(1-y)-(1-x^2)(1-y)-(1-x)(1-y^2)\},\\
N_4(x,y) &= \tfrac{1}{2}(1-x^2)(1-y),\\
N_5(x,y) &= \tfrac{1}{4}\{(1+x)(1-y)-(1-x^2)(1-y)-(1+x)(1-y^2)\},\\
N_6(x,y) &= \tfrac{1}{2}(1+x)(1-y^2),\\
N_7(x,y) &= \tfrac{1}{4}\{(1+x)(1+y)-(1-x^2)(1+y)-(1+x)(1-y^2)\},\\
N_8(x,y) &= \tfrac{1}{2}(1-x^2)(1+y).
\end{aligned}\right\} \tag{4.7}$$

Having constructed the interpolation functions $N_i(x,y)$ $(i = 1, 8)$ in an element, we can interpolate the whole domain in a straightforward manner, element by element. Approximating the continuous function $\phi(x,y)$ by the set of the discretized nodal values and a set of interpolation functions, we can find the stationary point of the functional defined in (3.14) with respect to all of the nodal values within the domain. We thus obtain the system of equations

$$\partial F/\partial \phi_i = 0 \quad (i = 1, N). \tag{4.8}$$

N is the total number of nodes; ϕ_i is the nodal value of ϕ at the ith node.

Let an element in R be R^e. Then we may decompose $F\{\phi\}$ as follows:

$$F\{\phi\} = \iint_R + \oint_C = \sum_e \left[\iint_{R^e} + \int_{C\cap C^e}\right] = \sum_e F^e\{\phi\}. \tag{4.9}$$

C^e represents the boundary of each R^e. The line integral is present only if the element has a boundary on which the boundary condition (3.2) is specified. We now approximate F^e within each element:

$$F^e\{\phi\} = F^e\{[N]\{\phi\}\}. \tag{4.10}$$

Henceforth we shall simply write F^e for the approximate value. As discussed in §3, it now becomes evident that the interpolation functions $N_i(x,y)$ must be chosen in conformity with the nature of the functional $F\{\phi\}$. In particular, they should be chosen so that, at the interfaces, the approximation to ϕ is continuous. This ensures that there is no contribution to the integral from the interfaces.

Then, from (4.8) and (4.9), we obtain

$$\frac{\partial F}{\partial \phi_i} = \sum_e \frac{\partial F^e}{\partial \phi_i} = 0. \tag{4.11}$$

For any nodal value we can write, by substituting (4.3) for each element and adding all the element integrals,

$$\frac{\partial F^e}{\partial \phi_i} = \iint_{R^e} \left(\phi_x \frac{\partial \phi_x}{\partial \phi_i} + \phi_y \frac{\partial \phi_y}{\partial \phi_i} + K_z^2 \phi \frac{\partial \phi}{\partial \phi_i} \right) dx\,dy + \int_{C \cap C^e} \left(p\phi \frac{\partial \phi}{\partial \phi_i} - q \frac{\partial \phi}{\partial \phi_i} \right) ds. \quad (4.12)$$

Noting that $\{\phi\}$ is no longer a function of x and y, but that $[N]$ is now a function of x and y, we obtain

$$\left.\begin{aligned} \frac{\partial \phi}{\partial x} &= \left[\frac{\partial N_i}{\partial x}, \frac{\partial N_j}{\partial x}, \ldots \right] \{\phi\}, \\ \frac{\partial \phi}{\partial y} &= \left[\frac{\partial N_i}{\partial y}, \frac{\partial N_j}{\partial y}, \ldots \right] \{\phi\}, \\ \frac{\partial}{\partial \phi_i} \left(\frac{\partial \phi}{\partial x} \right) &= \frac{\partial N_i}{\partial x}, \quad \frac{\partial}{\partial \phi_i} \left(\frac{\partial \phi}{\partial y} \right) = \frac{\partial N_i}{\partial y}, \\ \frac{\partial \phi}{\partial \phi_i} &= N_i. \end{aligned}\right\} \quad (4.13)$$

Finally, we obtain in the whole region

$$\frac{\partial F}{\partial \{\phi\}} = [A]\{\phi\} - [B] = 0, \quad (4.14)$$

or

$$[A]\{\phi\} = [B]. \quad (4.14')$$

The matrix $[A]$ and the column vector $[B]$ are defined, respectively, as

$$a_{ij} = K_{ij} + h_{ij}, \quad (4.15)$$

$$K_{ij} = \iint_R \left\{ \frac{\partial N_i}{\partial x} \frac{\partial N_j}{\partial x} + \frac{\partial N_i}{\partial y} \frac{\partial N_j}{\partial y} + K_z^2 N_i N_j \right\} dx\,dy,$$

$$= \sum_e \iint_{R^e} \left\{ \frac{\partial N_i}{\partial x} \frac{\partial N_j}{\partial x} + \frac{\partial N_i}{\partial y} \frac{\partial N_j}{\partial y} + K_z^2 N_i N_j \right\} dx\,dy, \quad (4.16)$$

$$h_{ij} = \int_C pN_i N_j ds = \sum_e \int_{C \cap C^e} pN_i N_j ds, \quad (4.17)$$

$$b_i = \int_C qN_i ds = \sum_e \int_{C \cap C^e} qN_i ds. \quad (4.18)$$

The formulated problem has now been reduced to (4.14'), a set of linear simultaneous algebraic equations. The coefficient matrix $[A]$ has the desirable properties of being symmetric, as one can see readily from (4.15)–(4.17), and of being banded if nodes are properly numbered. The actual numerical computations of the integrals (4.16)–(4.18) for general eight-node quadrilateral elements are made by Gaussian quadrature, having made a co-ordinate transformation into a square. A very extensive and detailed exposition of this method can be found in Zienkiewicz (1971).

A typical subdivision of meshes to solve a finite-depth problem is shown in figure 3, and is suitable for wavenumbers of the order $0 \lesssim Ka \lesssim 2$ in the beam sea case (i.e. $\alpha = 0°$).

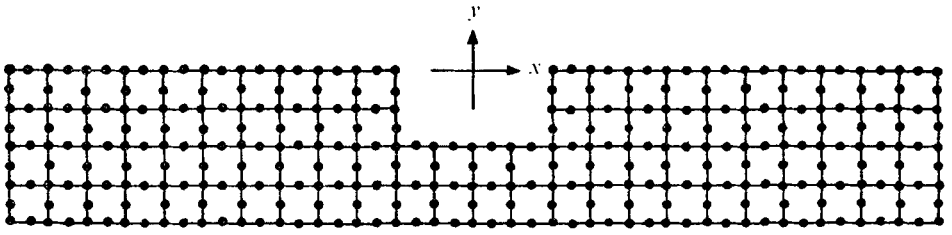

FIGURE 3. A typical subdivision of meshes for a finite-depth problem. $(H/b) = 2$. —•—, a node.

5. Results and discussion

Once the velocity potential is obtained, we can compute the linearized pressure by Bernoulli's equation

$$p = -\rho\Phi_t - \rho g y \tag{5.1}$$

(ρ and g are, respectively, the density of water and the acceleration of gravity), and the wave amplitude by the relation

$$\begin{aligned} Y(x,z,t) &= \mathrm{Re}\{-g^{-1}\,\Phi_t(x,0,z,t)\} \\ &= \mathrm{Re}\{Y_0(x,0)\exp(iK_z z - i\sigma t)\}. \end{aligned} \tag{5.2}$$

Of particular interest is the asymptotic wave amplitude

$$\overline{Y}_0 = \lim_{|x|\to\infty} |Y_0(x,0)|. \tag{5.3}$$

The local force and moment acting on a cross-section of the body are, respectively,

$$\mathbf{F} = \int_{C_B} p\mathbf{n}\,ds, \tag{5.4}$$

$$\mathbf{M} = \int_{C_B} p(\mathbf{r}\times\mathbf{n})\,ds. \tag{5.5}$$

$\mathbf{F} = (F_x, F_y)$; $\mathbf{r} = (x, y)$ the position vector; and $\mathbf{n} = (n_1, n_2)$ is the normal vector into the body. In §§ 5.1 and 5.2 we treat two specific problems that were analysed earlier by other authors.

5.1. *Heaving circular cylinder*

The problem considered in § 5.1 is a circular cylinder undergoing a small forced heaving (i.e. vertical) motion, such that the mean position of the centre of the circular cylinder is at the origin, and the heave motion is

$$\eta(z,t) = \mathrm{Re}\{\eta_0\exp(iK_z z - i\sigma t + i\tfrac{1}{2}\pi)\}. \tag{5.6}$$

In this case, the horizontal force and moment vanish owing to symmetry. The vertical force may be expressed in terms of non-dimensional coefficients: the added mass C_a and damping coefficient C_v. Following Ursell's definition, these are

$$C_a = -\int_{C_B} \mathrm{Re}\{\phi\}\,n_2\,ds/2a^2\eta_0\sigma, \tag{5.7}$$

$$C_v = -\int_{C_B} \mathrm{Im}\{\phi\}\,n_2\,ds/2a^2\eta_0\sigma; \tag{5.8}$$

		C_a		C_v		$\lvert\bar{Y}_0/\eta_0\rvert$	
Ka	α^0	This method	BU	This method	BU	This method	BU
0·25	5	0·6912	0·69	1·012	0·98	0·3410	0·35
	45	0·9307	0·93	1·3423	1·33	0·4797	0·48
	85	3·7331	3·72	0·9425	0·95	1·1636	1·16
1·25	5	0·4864	0·49	0·2272	0·22	0·8420	0·84
	45	0·4390	0·44	0·2055	0·20	0·9543	0·94
	85	0·7249	0·72	0·1028	0·11	1·9203	2·00
2·25	5	0·5605	0·57	0·0720	0·07	0·8441	0·84
	45	0·3225	0·33	0·0488	0·046	0·8340	0·81
	85	0·3728	0·37	0·0520	0·051	2·4496	2·42

TABLE 1. Comparisons of hydrodynamic coefficients and wave amplitudes obtained by the variational method with the results of BU (Bolton & Ursell 1973)

a is the half-beam of the cylinder. (Some authors use the submerged area in place of $2a^2$ in (5.7) and (5.8).) The hydrodynamic coefficients of more general cases are described in Wehausen (1971).

The added mass and damping coefficients and the non-dimensional asymptotic wave amplitude $\bar{Y}_0/\eta_0$ are computed for $Ka = 0{\cdot}25$, $1{\cdot}25$, and $2{\cdot}25$, and for the angles of obliquely propagating waves, generated by the heaving circular cylinder, of $\alpha = 5$, 45, 85°, respectively. Our computation is compared with the results of Bolton & Ursell (1973) in table 1. Agreement is in general good. If necessary, accuracy may be improved by taking finer meshes in the fluid region, and by using double precision in computation by a digital computer. An attempt was also made to compute the hydrodynamic coefficients for large Ka (viz. $Ka = 35$) as a test. One case (viz. $Ka = 35$ and $\alpha = 85°$) was tested: the added mass and damping coefficients were, respectively, 0·02192 and 0·00001075 (Bolton & Ursell (1973) give, respectively, 0·022 and 0·000016). Appendix B describes a modification of the numerical scheme for large Ka; a typical subdivision of meshes for this particular case is shown in figure 12.

5.2. *Wave diffraction by a rectangular cylinder*

In § 5.2 we discuss the problem of a plane wave incident upon a fixed rectangular cylinder of width $2a$ and draft b, as shown in figure 4. Our interests are the reflexion and transmission coefficients defined in (2.9), as well as the diffraction forces and moment. The non-dimensional forces and moment due to an incident wave of amplitude Y_I acting on a fixed body are defined, respectively, by

$$f_x = |F_x|_{\max}/\rho g Y_I a, \tag{5.9}$$

$$f_y = |F_y|_{\max}/\rho g Y_I a, \tag{5.10}$$

$$m_z = |\mathbf{M}|_{\max}/\rho g Y_I a. \tag{5.11}$$

For $a = 0$ (i.e. a vertical flat plate), a will be replaced by the half-draft $\frac{1}{2}b$.

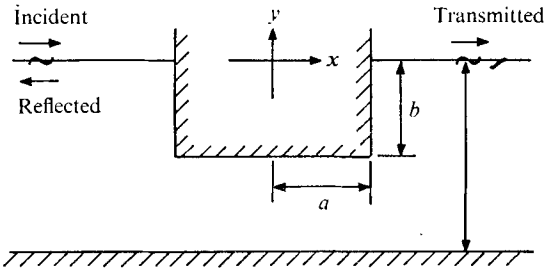

FIGURE 4. The configuration of the body geometry.

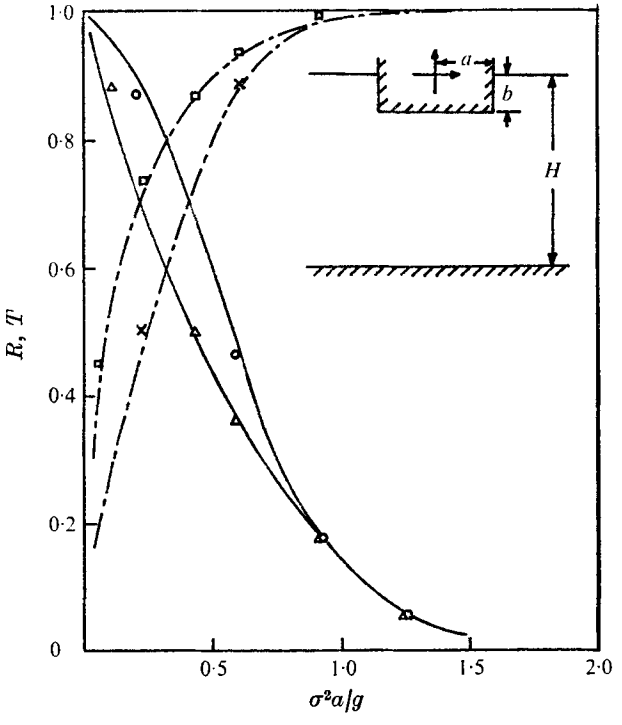

FIGURE 5. Coefficients for a rectangular cylinder in water of finite depth.

	$\alpha°$	Transmission T	Reflexion R
Variational method		———	– – – – –
Lebreton & Margnac	45	○	×
	75	△	□

The reflexion and transmission coefficients of the rectangular cylinder ($b/a = \frac{2}{3}$) in water of finite depth ($H/a = \frac{10}{3}$) were computed for the angles of incidence $\alpha = 45$ and 75°, and compared with the results of Lebreton & Margnac (1966) in figure 5. Agreement is good for $\alpha = 75°$, but not for $\alpha = 45°$ (when the non-dimensional wavenumber $\sigma^2 a/g$ is small).

The reflexion coefficient for a horizontal flat plate ($b = 0$) in water of infinite depth is compared with results of Garrison (1969) for $Ka = 0{\cdot}2$ and $Ka = 0{\cdot}4$

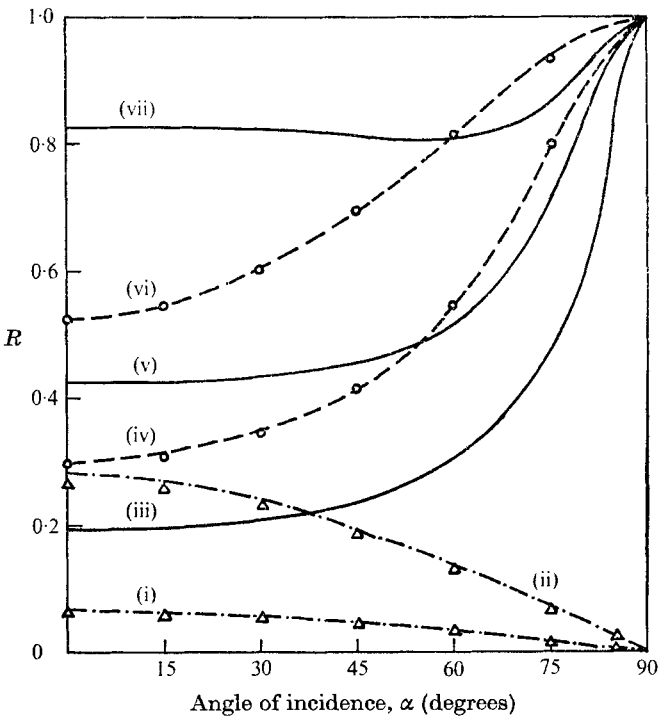

FIGURE 6. Reflexion coefficient in water of infinite depth. $b/a = \frac{2}{3}$, $H/a = \frac{10}{3}$.

	(i)	(ii)	(iii)	(iv)	(v)	(vi)	(vii)
Ka	0	0	0·1	0·2	0·2	0·4	0·4
Kb	0·2	0·4	0·1	0	0·2	0	0·4

Variational method —— ○ △ Garrison ------ Evans & Morris —·—·—

in figure 6. The corresponding non-dimensional force and moment acting on the flat plate, owing to the incident waves, are compared with results of Garrison (1969) in figures 7 (*a*), (*b*). Agreement is good in all three cases. For a vertical flat plate ($a = 0$), piercing the free surface, the reflexion coefficient, non-dimensional horizontal force and moment are shown in figures 6, 8 (*a*), (*b*), respectively. The reflexion coefficient is compared with results of Evans & Morris (1972) for $Kb = 0{\cdot}2$ and 0·4 in figure 6. At small angles of incidence, the reflexion coefficient of the vertical flat plate does not agree very well with the results of Evans & Morris (1972); agreement is improved as α approaches 90°. This may be due to the sinusoidal interaction mechanism of the strength of the square-root singularity, along the z axis, which is more significant as α approaches 90° (as discussed in appendix A).

To obtain more accurate information near the singularity, one can introduce more sophisticated interpolation functions that represent the singularity better than the simple polynomial interpolation functions we used in the present computation. The convergence of the finite-element method for problems with a

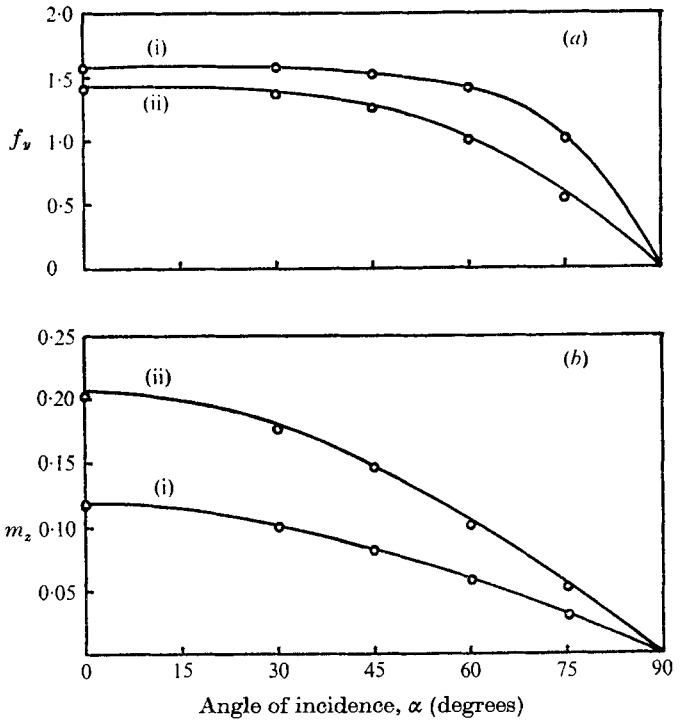

FIGURE 7. Non-dimensional (*a*) vertical force, (*b*) moment on a horizontal flat plate. $b/a = 0$, $H/a = \infty$. Ka: (i) 0·2, (ii) 0·4. ——, variational method; ○, Garrison.

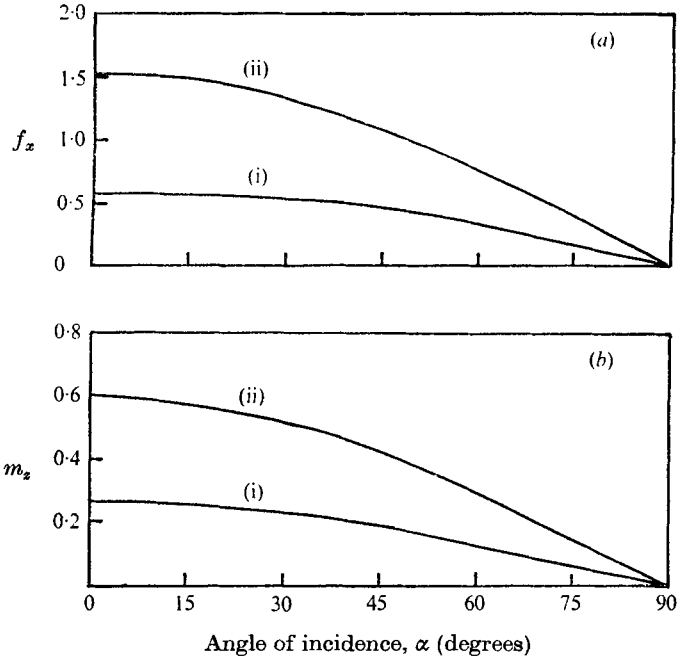

FIGURE 8. Non-dimensional (*a*) horizontal force, (*b*) moment on a vertical flat plate. $a/b = 0$, $H/b = \infty$. Kb: (i) 0·2, (ii) 0·4.

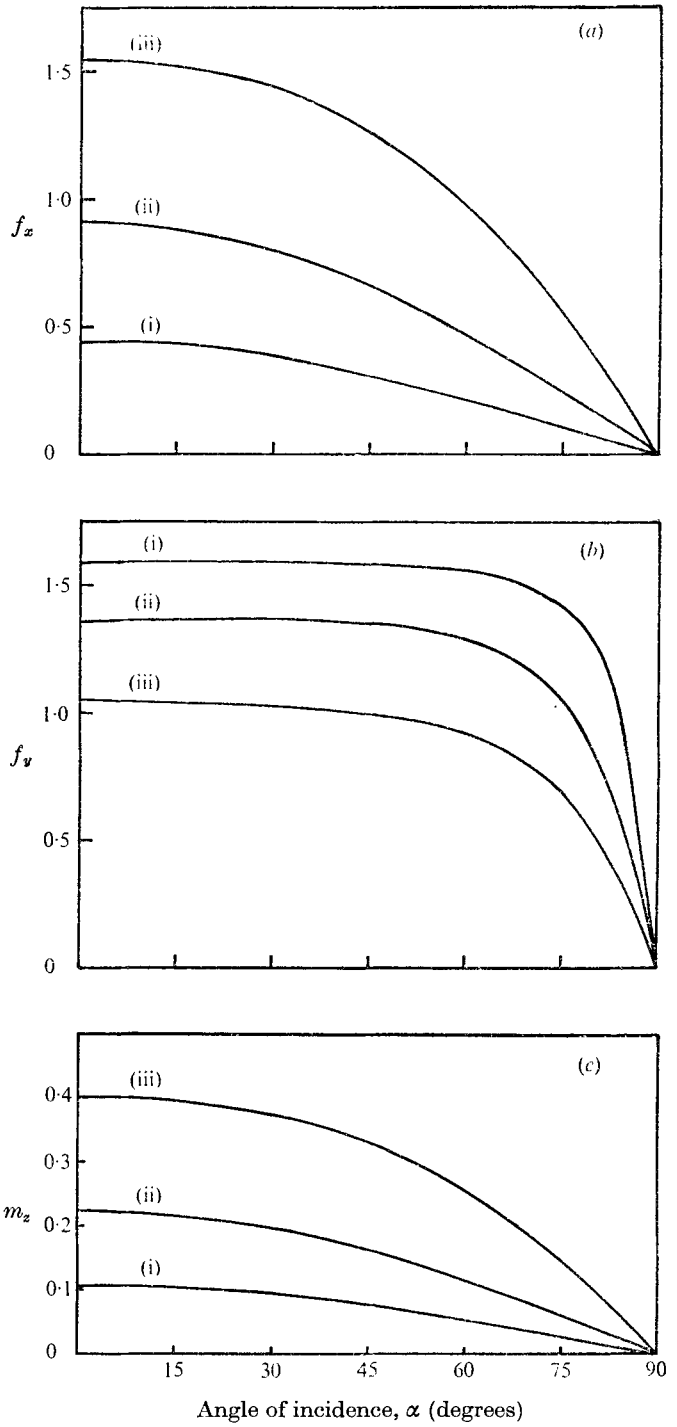

FIGURE 9. Non-dimensional (*a*) horizontal force, (*b*) vertical force, (*c*) moment on a rectangular cylinder in water of infinite depth. $b/a = 1$, $H/a = \infty$. Ka: (i) 0·1, (ii) 0·2, (iii) 0·4.

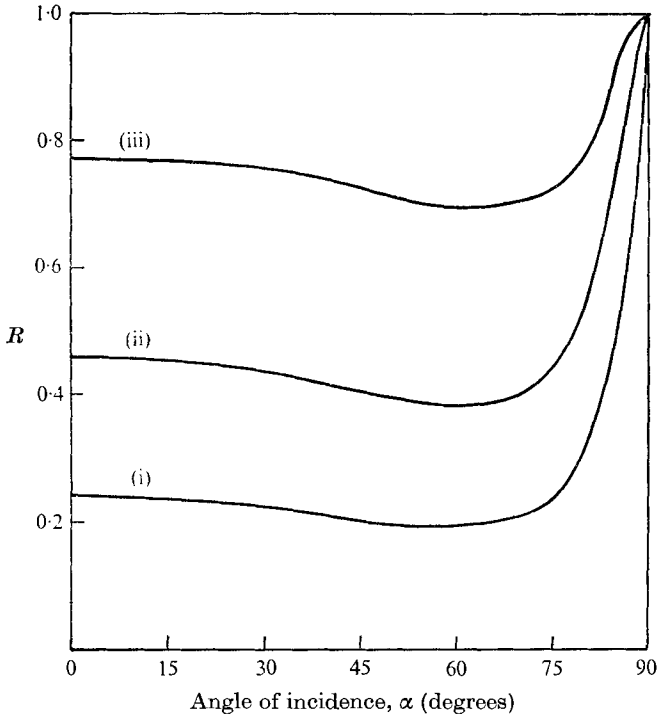

FIGURE 10. Reflexion coefficients of a rectangular cylinder in water of finite depth against angles of incidence. $b/a = 1$, $H/b = 2$. $Ka = Kb$: (i) 0·1, (ii) 0·2, (iii) 0·4.

singularity is treated in Tong & Pian (1973). The strength of the square-root singularity in cracked plates is also treated by the finite-element method in Yammoto & Tokuda (1973). A rigorous treatment of singularities in the finite-element method can be found in Strang & Fix (1973).

The reflexion coefficient, and the non-dimensional forces and moment for a fixed rectangular cylinder ($b/a = 1$), in water of infinite depth, are shown for $Ka = 0{\cdot}1$, 0·2 and 0·4 in figures 6 and 9(a)–(c). The reflexion coefficient, the non-dimensional forces and moment for a fixed rectangular cylinder, in water of finite depth ($h/a = 2$), are also shown for $Ka = 0{\cdot}1$, 0·2 and 0·4 in figures 10 and 11(a)–(c). For the cases $b/a = 1$, $b/a = 0$ and $a/b = 0$, the non-dimensional moment and the non-dimensional horizontal force (except for $b = 0$) are nearly constant up to a certain angle, then decrease to zero as the angle of incidence approaches 90°. For the limiting case $a = 0$, $b \neq 0$ (i.e. a vertical flat plate piercing the free surface), the reflexion and transmission coefficients, as shown by Evans & Morris (1972), are monotonic functions of the angle of incidence. The effect of finite angle is to reduce R and increase T. For an opposite limiting case $a \neq 0, b = 0$ (i.e. a horizontal flat plate on the free surface) R increases and T decreases with increasing α.

An eight-node quadrilateral element was used for the numerical computations. Computations were performed on the IBM 370 at the MIT Information Processing Center. The central processor time for each wavenumber was about 12 s

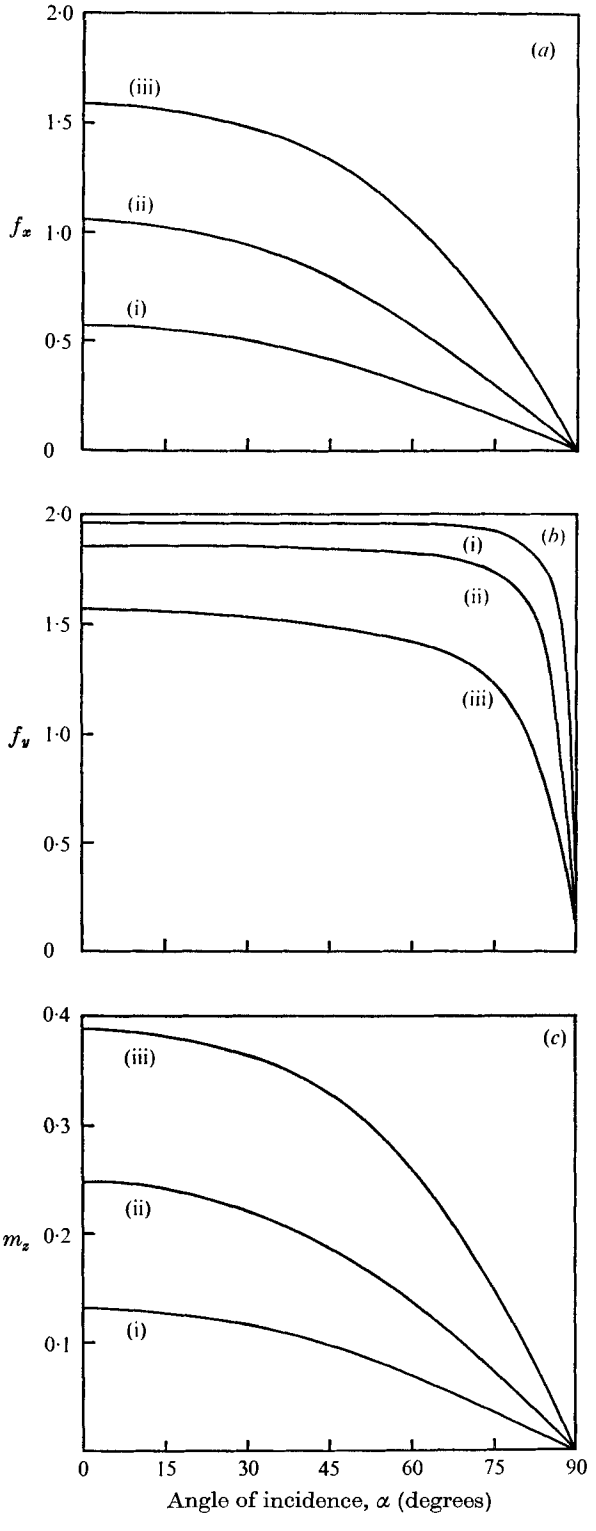

FIGURE 11. Non-dimensional (*a*) horizontal force, (*b*) vertical force, (*c*) moment on a rectangular cylinder in water of finite depth against angles of incidence. $b/a = 1, H/b = 2$. Ka: (i) 0·1, (ii) 0·2, (iii) 0·4.

for 88 elements and 325 nodes in the case of finite depth (figure 3), and about 22 s for 124 elements and 433 nodes for infinite depth. Both these cases are for the diffraction problem of a rectangle in oblique incident waves. Approximately 10 s were taken for 59 elements and 212 nodes for a forced-heave-motion problem of a circular cylinder. The main advantage of this method is that any complex geometry of the boundary can be easily accommodated: e.g. a bottom with variable depth (in the x, y plane) is no more difficult to analyse than one of constant depth.

The author is grateful to Professor J. N. Newman for suggesting this topic, and to Mr Kihan Kim for his assistance in the preparation of the computer program. This research was supported by the Office of Naval Research, contract N00014-67-A-0204-0023, and by the National Science Foundation, grant GK-10846.

Appendix A

To examine the behaviour of the local disturbance, we can use the eigenfunction expansions in water of finite depth. Then we can extend this result to the case of infinite depth, unless the angle α of the obliquely incident wave is zero.†

To find how fast the local disturbance of an oscillating body decays along the free surface, we construct two imaginary vertical boundaries, which extend from the bottom to the free surface, including any moving body in between. First we assume the depth is constant (i.e. $y = -H$). Then we can consider an infinitely-flexible-wall wave maker in a semi-infinite tank, which may be either of the two imaginary boundaries. In this wave-maker problem, we can assume that the solution is

$$\phi = \phi_p + \phi_L, \tag{A 1}$$

$$\phi_p = C_0 \cosh[m_0(y+H)\exp(iK_x x)], \quad x \geqslant 0, \tag{A 2}$$

$$\phi_L = \Sigma c_i \cos[m_i(y+H)\exp(-N_i x)], \quad x \geqslant 0, \tag{A 3}$$

with the relation

$$m_0 = K, \quad K_0 = -m_i \tan(m_i H), \quad N_i^2 = m_i^2 + K_z^2. \tag{A 4}$$

The coefficients C_0 and $C_i (i = 1, 2, \ldots)$ can be determined from the boundary condition on the wave maker; but we are not presently interested in finding them.

Since N_1 is the smallest eigenvalue and accordingly gives a component of the slowest decay among all possible components of the local disturbance, we define the decay factor

$$d(x) \equiv \exp(-N_1 x). \tag{A 5}$$

† When $\alpha = 0°$, this problem is reduced to a strictly two-dimensional problem in water of infinite depth. In this case we cannot use the eigenfunction expansion; instead we use a pulsating source. When α is small, even if not zero, we cannot in general obtain useful information for the truncation of the infinite boundary, to find the optimum distance for the numerical scheme.

From the well-known relation

$$\tfrac{1}{2}\pi < m_1 H < \pi, \tag{A 6}$$

we have

$$N_1^2 = m_1^2 + K_z^2 > K_z^2 + [\pi/(2H)]^2. \tag{A 7}$$

From (A 5) and (A 7), we have

$$d(x) < \exp[-\{K_z^2 + [\pi/(2H)]^2\}^{\frac{1}{2}} x]. \tag{A 8}$$

The local disturbance always decays faster than $d(x)$. Therefore we can use $d(x)$ as a criterion to truncate the infinite boundary, and construct a 'new boundary' on which the radiation condition (2.21) is to be imposed in the numerical scheme.

Let us consider two examples. (i) When $K_z \ll \pi/(2H)$, we have

$$N_1 \cong \pi/(2H), \quad N_1 > \pi/(2H); \tag{A 9a, b}$$

and we obtain an inequality

$$d(x) < \exp[-\pi x/(2H)]. \tag{A 10}$$

The relation (A 10) shows that the local disturbance is reduced to, at least, $\exp(-2\pi)$ times its value at the wave maker (i.e. $x = 0$), when we take the distance from the wave maker equal to four times the depth.

(ii) When the depth H becomes very large, such that $K_z \gg \pi/(2H)$, we have a relation for the decay factor

$$d(x) \cong \exp(-K_z x), \quad d(x) < \exp(-K_z x). \tag{A 11a, b}$$

Relation (A 11) shows that, if $K_z = 1\ (m^{-1})$, then the decay of the local disturbance is at least as small as $\exp(-2\pi)$ times its value on the wave maker when we take $x = 2\pi\,(m)$, where K_z is the z component of the wavenumber. This (rather crude) criterion is useful in finding an optimum distance† for truncating the infinite boundary. When this criterion gives too large a distance, or when we do not have an appropriate criterion, it is necessary to use a trial-and-error method of testing several different distances. Also, a local disturbance decays faster as α increases when K is fixed, i.e. the local disturbance vanishes more rapidly in oblique waves ($\alpha > 0$) by comparison with the beam sea case ($\alpha = 0$). Presumably this is due to the interaction along the z axis and resulting cancellation of the local disturbance. Bai (1972) discussed the behaviour of local disturbances in water of infinite depth in two dimensions ($\alpha = 0$).

Appendix B

In water of infinite depth, when Ka is very large, a slight modification is necessary to construct the radiation and bottom boundaries for numerical computation. We consider here a particular case: $Ka = 35$ and $\alpha = 85°$. For simplicity, we assume $a = 1$ (m). Then we have

$$K = 35\,(\mathrm{m}^{-1}) \text{ and } K_z = 35 \sin 85° \cong 35.$$

† The optimum distance from the body is large enough to neglect the local disturbance, and small enough to solve economically, and to neglect the significant accumulation of round-off errors.

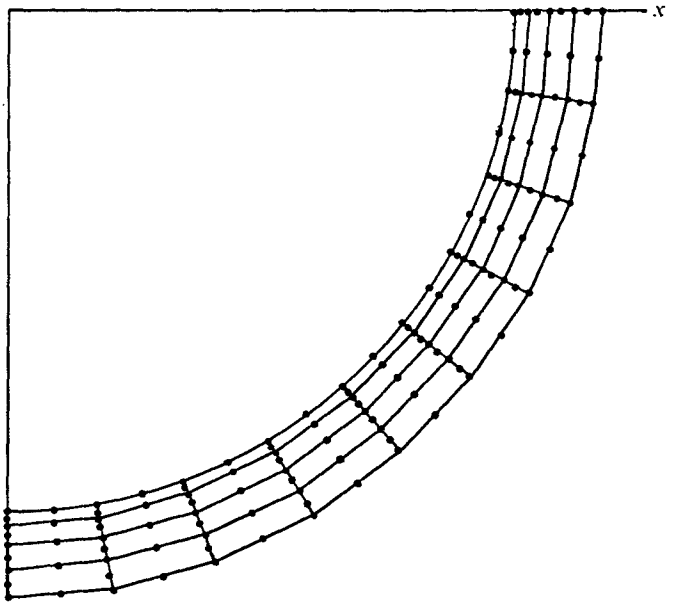

FIGURE 12. A typical subdivision of meshes for a circular cylinder on the free surface. $Ka = 35$, $\alpha = 85$.

The wavelength is $2\pi/K \cong 0{\cdot}18$ (m). From (A 11), the local disturbance is at least as small as $\exp(-2\pi)$ times its value at the intersection of the circular cylinder and the free surface, when we consider the potential at one wavelength (i.e. 0·18 m) from this point on the free surface. If we had examined the behaviour of the local disturbance, by making use of the eigenfunction expansion in the polar co-ordinate, we might have obtained the decay factor defined in appendix A in terms of radius r and angle α, rather than x, along the free surface. Hereafter, we conjecture that the local disturbance decays approximately in a similar fashion in all radial directions in the fluid, as in the relation (A 11). It should be noted that the apparent wavelength in the x, y plane ($2\pi/K_x$) is much larger than the real wavelength of 0·18 m.

If the local disturbance is confined to a thin layer along the cylinder, we may attempt to construct a new boundary condition along a fictitious circular boundary which encloses the local disturbance. We can easily construct the required boundary condition, making use of the normal vector $\mathbf{n} = (n_1, n_2)$, pointing outward on the fictitious boundary, say the outer circle. It can be expressed as

$$\partial\phi/\partial n - n_2 K_0 \phi = i n_1 K_x \phi. \tag{B 1}$$

K_0 and K_x are as defined earlier. A detailed derivation of the relation (B 1) is given by Bai (1972). As an illustration, the subdivision of the meshes for $Ka = 35$ and $\alpha = 85°$ is shown in figure 12.

REFERENCES

BAI, K. J. 1972 A variational method in potential flows with a free surface. Ph.D. dissertation, Department of Naval Architecture, University of California, Berkeley.

BLACK, J. L. & MEI, C. C. 1970 Scattering and radiation of water waves. *Water Resources and Hydrodynamics Laboratory, Department of Civil Engineering, Massachusetts Institute of Technology, Rep.* no. 121.

BOLTON, W. E. & URSELL, F. 1973 The wave force on an infinitely long circular cylinder in an oblique sea. *J. Fluid Mech.* **57**, 241–256.

EVANS, D. V. & MORRIS, C. A. N. 1972 The effect of a fixed vertical barrier on obliquely incident surface waves in deep water. *J. Inst. Math. Appl.* **9**, 198–204.

GARRISON, C. J. 1969 On the interaction of an infinite shallow draft cylinder oscillating at the free surface with a train of oblique waves. *J. Fluid Mech.* **39**, 227–255.

LEBRETON, J. C. & MARGNAC, M. A. 1966 Traitement sur ordinateur de quelques problèmes concernant l'action de la houle sur les corps flottants en theorie bidimensionelle. *Bulletin du Centre de Recherches et D'Essais de Chatou*, no. 18, 3–43.

MEI, C. C. & BLACK, J. L. 1969 Scattering of surface waves by rectangular obstacles in waters of finite depth. *J. Fluid Mech.* **38**, 499–511.

STRANG, G. & FIX, G. 1973 *An Analysis of the Finite Element Method.* Prentice-Hall.

TONG, P. & PIAN, T. H. H. 1973 On the convergence of the finite element method for problems with singularity. *Int. J. Solid Structures*, **9**, 313–321.

WEHAUSEN, J. V. 1971 The motion of floating bodies. *Ann. Rev. Fluid Mech.* **3**, 237–268.

YAMAMOTO, Y. & TOKUDA, N. 1973 Determination of stress intensity factors in cracked plates by the finite element method. *Int. J. Numerical Method Engng*, **6**, 427–439.

ZIENKIEWICZ, O. Z. 1971 *The Finite Element Method in Engineering Science.* McGraw-Hill.